

Quantitative Colorimetric Detection of Dissolved Ammonia Using Polydiacetylene Sensors Enabled by Machine Learning Classifiers

Papaorn Siribunbandal, Yong-Hoon Kim, Tanakorn Osotchan, Zhigang Zhu, and Rawat Jaisutti*

Cite This: *ACS Omega* 2022, 7, 18714–18721

Read Online

ACCESS |



Metrics & More

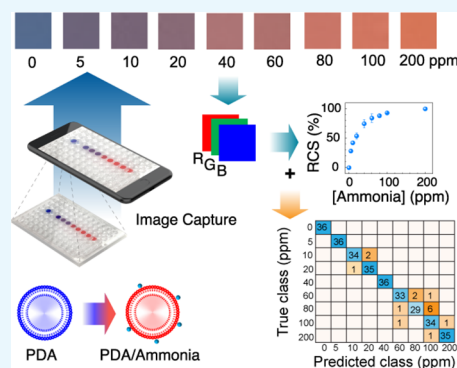


Article Recommendations



Supporting Information

ABSTRACT: Easy-to-use and on-site detection of dissolved ammonia are essential for managing aquatic ecosystems and aquaculture products since low levels of ammonia can cause serious health risks and harm aquatic life. This work demonstrates quantitative naked eye detection of dissolved ammonia based on polydiacetylene (PDA) sensors with machine learning classifiers. PDA vesicles were assembled from diacetylene monomers through a facile green chemical synthesis which exhibited a blue-to-red color transition upon exposure to dissolved ammonia and was detectable by the naked eye. The quantitative color change was studied by UV–vis spectroscopy, and it was found that the absorption peak at 640 nm gradually decreased, and the absorption peak at 540 nm increased with increasing ammonia concentration. The fabricated PDA sensor exhibited a detection limit of ammonia below 10 ppm with a response time of 20 min. Also, the PDA sensor could be stably operated for up to 60 days by storing in a refrigerator. Furthermore, the quantitative on-site monitoring of dissolved ammonia was investigated using colorimetric images with machine learning classifiers. Using a support vector machine for the machine learning model, the classification of ammonia concentration was possible with a high accuracy of 100 and 95.1% using color RGB images captured by a scanner and a smartphone, respectively. These results indicate that using the developed PDA sensor, a simple naked eye detection for dissolved ammonia is possible with higher accuracy and on-site detection enabled by the smartphone and machine learning processes.



1. INTRODUCTION

Detection of dissolved ammonia is significantly essential for managing aquatic ecosystems and aquaculture products since excessive emission of ammonia could deteriorate water quality and be harmful to many species of aquatic life.¹ The ammonia contamination in an aquatic environment may come from domestic, agricultural, and industrial effluents owing to a rapid increase of urbanization and industrialization. It has been reported that the production of greenhouse gas—nitrous oxide—has been found in the oceans, which occurs by ammonia-oxidizing archaea under hypoxic conditions.² In addition, oxidation of ammonia to cancerogenic nitrate by nitrobacteria can cause health risks for longtime drinking of ammonia-containing water.³ It is recommended that the final acute ambient water quality criterion for protecting freshwater organisms from the potential effects of ammonia is 17 ppmv total ammonia nitrogen.⁴ Therefore, a simple and low-cost ammonia detector is of great demand for rapid on-site testing and continuous monitoring of water quality.

Numerous analytical techniques are available for the analytical detection of ammonia in water, such as ion-selective electrodes,^{5,6} electrochemical analyses,⁷ and conductometric⁸ and fluorescence spectroscopies.^{9,10} These methods can precisely analyze ammonia quantitatively; however, they are rather time-consuming and costly and require complex instrumentation. Therefore, the development of a colorimetric

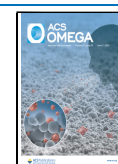
sensor, which is easy-to-use and of low cost and has a convenient readout with the naked eye, is of great interest. Several studies have been carried out on colorimetric detection of ammonia using different sensing materials, such as carbon dots,³ indophenol blue,¹¹ and bromothymol blue.¹² However, most of the reported methods are based on spectrophotometry of Nessler's^{5,13} and Berthelot's^{14–16} reactions, which exhibit low sensitivity and poor selectivity or use of a toxic reagent. Also, some of the samples must be purified before determination of ammonia; otherwise, some dissolved alkaline species can interfere with the measurements.^{11,17} In addition, commercially available test methods are relatively expensive and can interfere with ions, suspended solids, and colored compounds.^{10,12}

Polydiacetylenes (PDAs), conjugated polymers, are one of the attractive materials for various colorimetric sensing applications, including organic solvents,¹⁸ temperature,¹⁹ pHs,^{20,21} and biomarkers.^{22,23} The color change of PDAs

Received: March 9, 2022

Accepted: May 12, 2022

Published: May 26, 2022



from blue to red upon exposure to stimuli is due to the conformational transition of the PDA backbone from planar to non-planar. One of the most critical features of PDAs is that their building blocks can be locally functionalized and chemically modified, making them possess tunable sensitivities to stimuli.²⁴ PDAs undergo a color change when exposed to ammonia. However, none of these studies developed PDA hybrid films that detect ammonia in the gas phase.^{25–27} Based on our knowledge, there are still no reports on PDA-based colorimetric sensors for dissolved ammonia detection. Although the visible blue-to-red color change of PDA-based sensors can be observed by the naked eye and easily understood by non-specialists, however, there are deficiencies in quantification and precision. Therefore, smartphone technologies^{28,29} or scanner platforms¹⁸ were used to extract the quantitative data from color images. The color change of PDAs can be quantified using the red–green–blue (RGB) (red, green, and blue) color space of the taken images and applying a simple analytical model such as the red chromatic shift (RCS)¹⁸ and red–blue ratios.²⁵

In order to convert colors to analytical values, the methods mentioned above use JPEG images to obtain a calibration curve. However, the JPEG images are compressed files, and their quality depends on device proprietary software, making the final analytical data not completely reliable.^{30,31} In addition, colorimetric analysis is susceptible to ambient light conditions, smartphone brands, and camera optics. Therefore, machine learning algorithms were proposed as intelligent systems for the quantitative analysis process.^{31–33} The pre-obtained images were used to train the learning model and automatically perform colorimetric tests as new data arrived. In particular, machine learning is now widely used in sensor applications and automatic systems, owing to its powerful utilities such as self-learning from the training data and self-automated decisions from the learned database.³² The flexibility and adaptability to new machine learning platforms, such as smartphone-based systems^{33,34} and embedded systems,^{35,36} lead to a reliable quantitative and qualitative evaluation of colorimetric analysis.

In this work, easy-to-use detection of dissolved ammonia was developed using the PDA vesicles which were assembled from a diacetylene monomer through facile green chemical synthesis. Upon a fine control of the synthesis process and polymerization conditions, the blue-to-red color change of the PDA sensor was observed by the naked eye when exposed to ammonia. Quantitative analysis of ammonia concentrations was performed using UV–vis spectroscopy and digital colorimetric analysis with machine learning classifiers. A support vector machine (SVM) was used as the learning model for classifying the sample color images obtained from a scanner and a smartphone under different ammonia concentrations. The results showed that our colorimetric detection system possessed excellent quantitative detection of dissolved ammonia with a detection limit of 10 ppm. It indicates that the proposed PDA sensor-integrated machine learning platform can be potentially utilized as a portable intelligent system with high accuracy, convenient on-site detection, and real-time ammonia monitoring.

2. EXPERIMENTAL SECTION

2.1. Preparation of PDA Vesicles. Diacetylene monomer 10,12-pentacosadiynoic acid (PCDA) (>97%) was purchased from Sigma-Aldrich. Ethanol was received from RCI Labscan

Limited, Thailand. Aqueous ammonia solution (25%) with an assay of 99.9% was purchased from Merck. All chemicals used in this work were of analytical reagent grade and used as received. The PDA vesicles were synthesized using a facile green chemical process. Briefly, the diacetylene monomer PCDA was dissolved in 10 mL of ethanol and filtered using a 0.45 μm pore size nylon membrane to remove any contaminant. The ethanol solvent was slowly evaporated under a controlled temperature of 80 $^{\circ}\text{C}$ under continuous magnetic stirring. Then, deionized water was added to yield a suspension concentration of 0.5 mM and continuously stirred at 80 $^{\circ}\text{C}$ for 90 min to remove the residual ethanol. The resulting translucent solution was cooled down to room temperature and stored in a refrigerator at 4 $^{\circ}\text{C}$ for 18 h. After that, the self-assembled PCDA was irradiated by a UV light (UV lamp OSRAM, PHILIPS, TOKIVA) at a wavelength of 254 nm (light intensity 1.5 mW cm^{-2}) for 5 min under magnetic stirring. Finally, a dark blue suspension of PDA vesicles was obtained, which was used freshly as prepared or after storing at 4 $^{\circ}\text{C}$ with light protection until use. To optimize the sensing performance, the PDA sensors have been developed by adjusting the concentrations of PCDA in the suspension as follows: 0.25, 0.5, 0.75, 1.0, and 1.5 mM.

2.2. Characterization of PDA Vesicles. The PDA vesicles before and after ammonia exposure were characterized using Fourier transform infrared (FTIR) spectroscopy (Bruker model Vertex 70) with an attenuated total reflection setup. The samples were prepared by drop-casting onto a cellulose paper and drying at room temperature. The morphology of the PDA vesicles in the dried state was examined using scanning electron microscopy (SEM, JEOL JSM-6400). Dynamic light scattering (DLS) analysis (Zetasizer nano ZS, Malvern Instruments) was conducted to confirm the size distribution of the PDA vesicles. DLS measurements were performed using samples without dilution. In addition, the optical absorption spectra were measured using a UV–vis spectrometer (Thermo Scientific, Genesys 10 Series).

2.3. Colorimetric Response Analysis of the PDA Sensor. The colorimetric response (CR) of PDA sensors to different ammonia concentrations was explored by adding the PDA vesicles into ammonia-dissolved water. The mixed solution was then incubated at room temperature, and its color change was monitored using optical absorption spectroscopy and digital colorimetric analysis. Based on the optical absorption analysis, a blue-to-red color transition of PDA sensors was evaluated as a CR according to $\text{CR}(\%) = [(PB_0 - PB)/PB_0] \times 100$. PB_0 and PB are the relative ratios of blue and red elements in the absence and presence of ammonia, respectively. PB can be calculated from $A_{\text{blue}}/(A_{\text{blue}} + A_{\text{red}})$, where A_{blue} and A_{red} are the absorbance of blue ($\lambda = 640 \text{ nm}$) and red ($\lambda = 540 \text{ nm}$) phases of the PDA sensor, respectively.

For digital colorimetric analysis, a 96-well plate containing the test solutions (300 μL) was scanned in the transmitted mode using a flatbed scanner (Epson Perfection V370 Photo Scanner). The scanner was set to produce 800 dots-per-inch (dpi) 24-bit color depth RGB images (TIF format). In addition, digital colorimetric analysis has also been done using images taken by a smartphone (iPhone SE) located 30 cm away from the samples under scanner light illumination. The smartphone camera was used in the manual mode with 1.8 focus level, 1/100 s shutter speed, 80 ISO level, and white balance kept constant throughout the experiments.

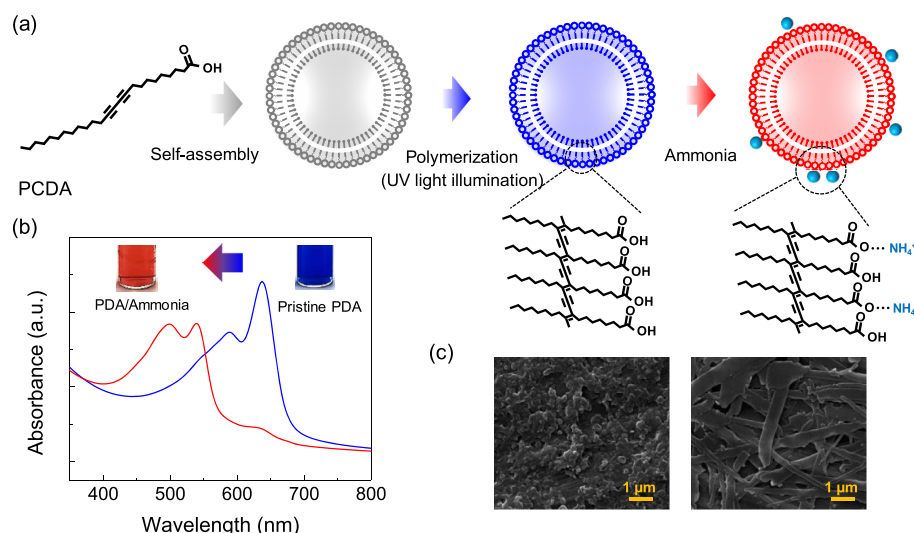


Figure 1. (a) Schematic illustration of the preparation of PDA vesicles from PCDA and their sensing mechanism for ammonia detection. (b) UV-vis absorption spectra and (c) SEM images of PDA before and after exposure to 100 ppm ammonia.

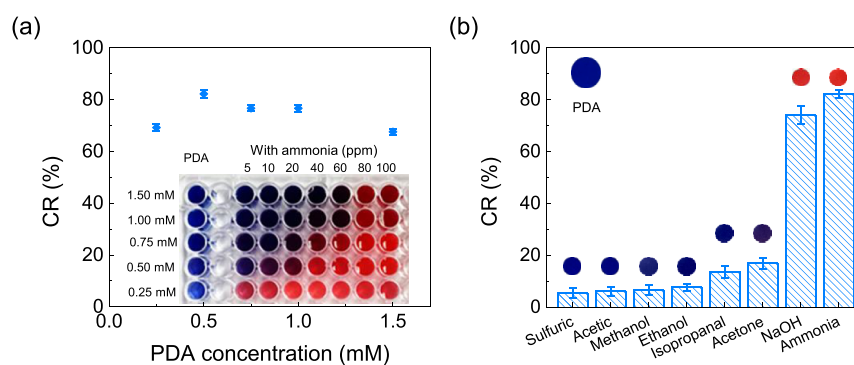


Figure 2. CR of (a) PDA with different PCDA concentrations and in the presence of 100 ppm concentration of ammonia and (b) PDA (0.5 mM) sensing system after the addition of various solvents with the concentration of 1000 ppm compared to 100 ppm ammonia. Insets are the corresponding photographs of a PDA sensing system.

2.4. Machine Learning Classifier. An SVM was used to train and evaluate the ammonia concentration from the colorimetric levels of different reagents to identify the correlation between the color change and ammonia concentration. The data set consists of 9 testing sets for the 9 distinct different ammonia concentrations (0–200 ppm), and 12 selected areas were extracted for each sample image. In addition, an average of R, G, and B color channels and RCS values for each spot image were extracted and used as the features to train the classifier in MATLAB (R2021a, Mathwork Inc, USA).

3. RESULTS AND DISCUSSION

3.1. PDA Sensing Mechanism. PDA-based sensors were synthesized using a facile green chemical process for colorimetric detection of dissolved ammonia. In particular, polymerization of PDA vesicles was induced by irradiating UV light to self-assembled PCDA monomers, forming a visible blue color PDA solution as shown in Figure 1a. The corresponding optical absorption spectra of the blue-phase PDA vesicles indicate a typical peak at 640 nm with a broad shoulder at 590 nm (Figure 1b). Notably, a blue-to-red color change occurs when the PDA sensor was exposed to dissolved ammonia. This color change was confirmed spectroscopically as the absorption signal at 640 nm decreased and the emergent

absorption signal at 540 nm increased. With the blue-to-red color transition, the size and morphology of PDA vesicles were obviously changed. According to DLS analysis, the pristine PDA vesicles had an average diameter of ~ 220 nm, and the particle size could not be detectable after the addition of ammonia solution. The SEM images confirmed that the PDA vesicles have a similar average particle size to the DLS data for the pristine sample (Figure 1c), and their morphology was changed to a line-like structure after the addition of ammonia in the solution. This result can be attributed to the aggregation of spherical PDA vesicles, forming larger size PDA lines.^{37,38}

FTIR spectroscopy was also used to study the blue-to-red colorimetric transition of the PDA-based sensors (Figure S1). When ammonia was added into the PDA solution, a new peak was generated at 1520 cm^{-1} , and a broad absorption peak was observed at around 1640 cm^{-1} , which can be assigned to the hydrogen-bonded carbonyl stretching of the carboxylate ($-\text{COOH}$) groups of PDA.³⁹ The color change of PDA in the presence of ammonia is mainly due to the interaction between the $-\text{COOH}$ groups of PDA and the amine groups of ammonia.^{25,38} The electrostatic interaction between the carboxylate anion (COO^-) and ammonium cation (NH_4^+) causes a relaxation of PDA backbones, resulting in a color change from blue to red.^{38,40} The complete color change indicates the absence of hydrogen bonding interactions.^{25,39}

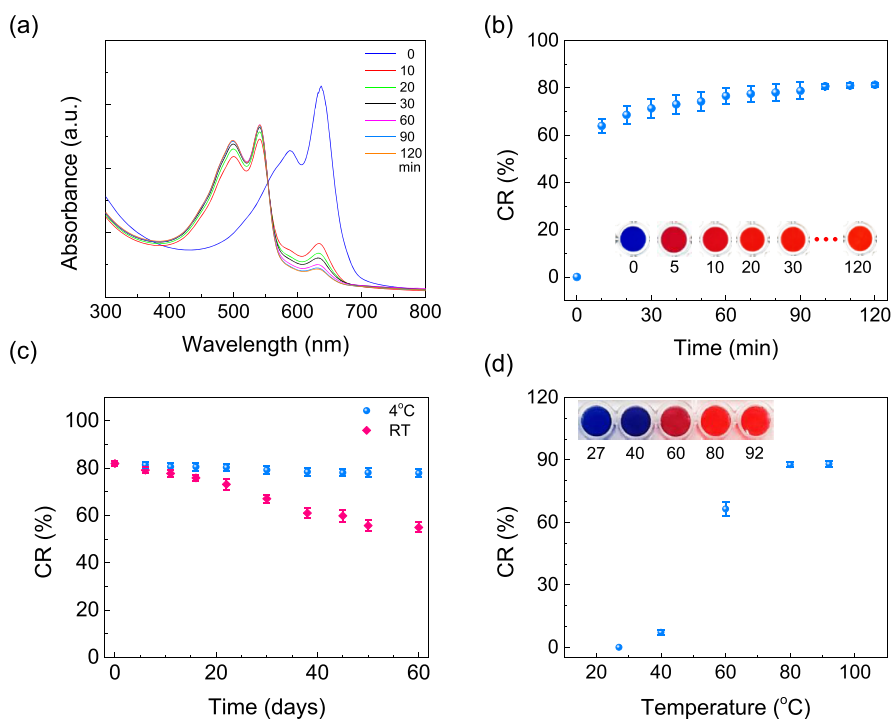


Figure 3. Time-dependent (a) UV–vis absorption spectra and (b) corresponding CR of PDA vesicles in the presence of 100 ppm ammonia concentration. CR of PDA samples: (c) storage in a refrigerator and room temperature for 60 days and (d) test under stimulating different temperatures. The insets show the photographs of PDA solution under other stimuli.

To obtain high sensitivity and reliable sensing performance, the concentration of the PCDA monomer in the PDA sensor system was first optimized. The CR of PDA sensors to dissolved ammonia (0–100 ppm) was analyzed, as shown in Figure 2a, with the PCDA concentration varied in the range of 0.25–1.5 mM. In all PCDA monomer concentrations, the color transitions from blue to purple and red could be observed with different thresholds. In particular, when the PCDA monomer concentrations were 1.0 and 1.5 mM, the color transition occurred at relatively high ammonia concentrations (≥ 60 ppm). In comparison, 0.25 mM PCDA exhibited a color transition from blue to red at a lower ammonia concentration of 5 ppm (inset of Figure 2a). In the case of 0.75 mM PCDA, a gradual blue to red color change was clearly observed for the ammonia concentration higher than 40 ppm. Also, 0.5 mM PCDA exhibited a wider color transition range from blue to red, as illustrated in the inset of Figure 2a. In the tested PCDA concentration range, the percentage of CR to 100 ppm ammonia was highest with 0.5 mM PCDA. Therefore, the optimized concentration of our PDA sensors for ammonia detection was set to 0.5 mM PCDA monomer.

To examine the selectivity of PDA sensors to ammonia, the CR to other solutions, including methanol, ethanol, isopropanol, acetone, acetic acid, sulfuric acid, and sodium hydroxide, was investigated. The concentrations of such solutions were 10 times higher than that of ammonia. As shown in Figure 2b, other solutions had limited effects on the color change of PDA. In particular, the PDA sensor exhibited a CR of $78.83 \pm 1.45\%$ for 100 ppm of ammonia, almost 6 times higher than other test solutions (Figure S2). These results clearly show that the PDA sensors have a high selectivity to ammonia owing to the strong interaction between the carboxylate ion of PDA and ammonia cation. In the case of alcohol, the hydrogen bonding between their polar –OH

group and –COOH groups of PDA has weakened inter-chain interactions, leading to a low level of color change.²⁵ The PDA sensor exhibits no color change for testing with acidic solutions; however, the sensor has response to the strong base solution, which may affect the performance of the sensor.

3.2. Sensing Characteristics. Time-dependent light absorption changes under ammonia exposure with a concentration of 100 ppm are shown in Figure 3a, and its corresponding CRs are shown in Figure 3b. The blue to red color transition occurred rapidly, and the response was saturated within a detection time of ~ 20 min. After saturation, the responses were maintained at a nearly constant level for 2 h, which can be attributed to the irreversible nature of the sensing reactions. Nonetheless, a detection time of 20 min can be an acceptable timescale for on-site ammonia detection of water samples. In addition, the sensing stability has been investigated by keeping the PDA solution in a sealed dark bottle and storing it at a relatively low temperature (4 °C) and ambient environment (30–35 °C, 55–60% RH). It was found that the PDA sensors could be stably stored for 60 days in a refrigerator (4 °C) with good CRs as shown in Figure 3c. In contrast, the sensor showed degradation in CR when it was stored in an ambient environment. The CR value of the sensor decreased ~ 5 and $\sim 33\%$ after storing in a refrigerator for 60 days and at an ambient environment, respectively. Therefore, the PDA solutions should be sealed and stored at a relatively low temperature to maximize the color rendering effect for an extended shelf life.

The PDA-based sensors were further characterized by heating in a hot water bath to study their thermochromic response. The optical absorption spectra and photographs of the PDA sensors at temperatures ranging from room temperature (27 °C) to 92 °C are shown in Figures 3d and S3, respectively. The results show that the PDA sensors first

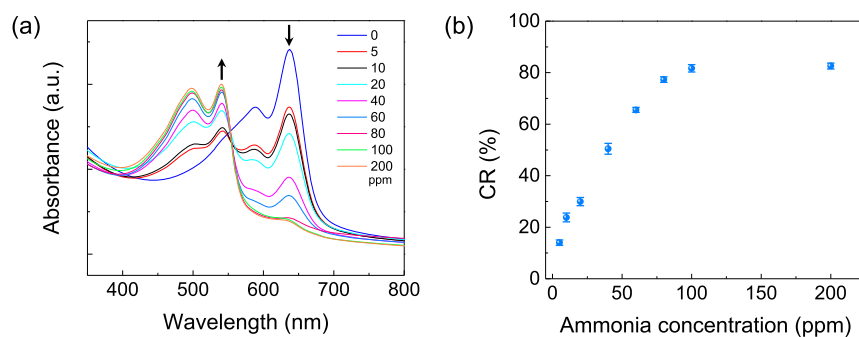


Figure 4. (a) Optical absorption spectra and (b) CR of PDA sensing system after incubation with different concentrations of ammonia in the range of 5–200 ppm.

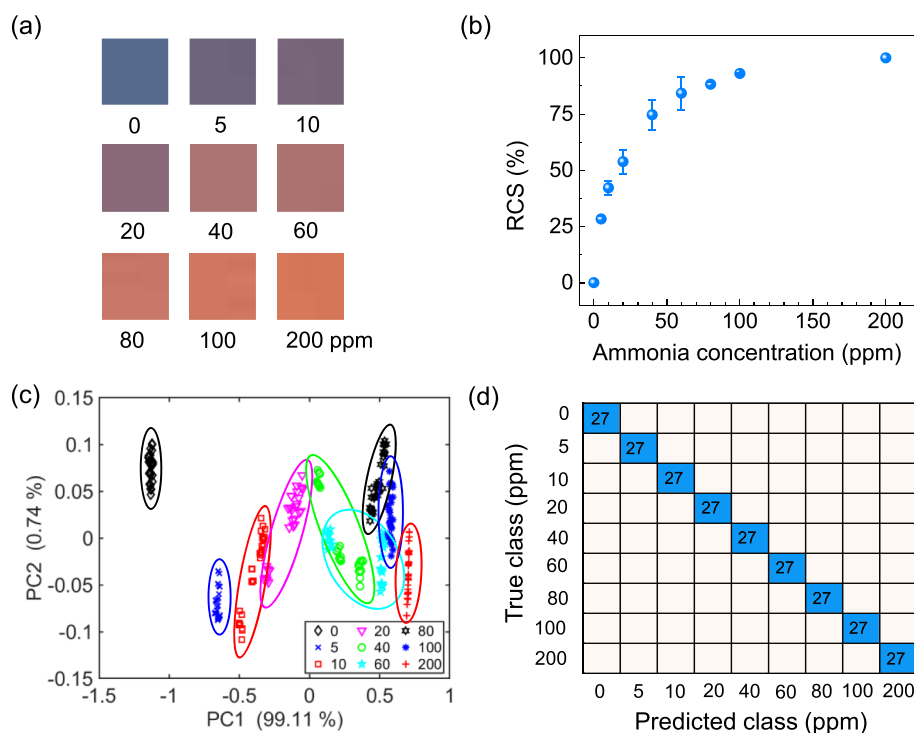


Figure 5. CR of the PDA sensor in the presence of different ammonia concentrations in the range of 5–200 ppm: (a) scanner images, (b) red CR, (c) PCA score plot of the first two PCs, and (d) confusion matrix of an SVM classifier.

underwent a significant color change starting at around 40 °C with the CR increasing to 10%. Furthermore, when the heating temperature was increased to 60 °C, the red color transition was observed (Figure 3d). These results suggest that the PDA sensor for ammonia detection should be carried out near room temperature to eliminate the influence from the thermal-induced color transition. For the thermal-induced color transition of PDA-based sensors, it is expected that the PDAs gain sufficient energy for structural rearrangement and rotation around the conjugated bonds, which alter the effective conjugation length prompting an irreversible blue to red change.

Next, the variation of CR s of PDA sensors to different ammonia concentrations was analyzed in the range of 5–200 ppm. Here, solutions containing PDA vesicles and ammonia were incubated, and their UV absorption was measured. As shown in Figure 4a, the absorption signal at 640 nm gradually decreased with increasing ammonia concentration, accompanied by an increase of a new absorption band at around 540 nm. The CR s show an almost linear increase of ammonia

concentration in the range of 5–80 ppm ($y = 0.847x + 12.355$, $R^2 = 0.9867$) (Figure 4b). The CR was nearly unchanged once the concentration was higher than 80 ppm. The limit of detection (LOD) was calculated based on the standard deviation (σ) of the response and the slope of the curve (S) according to $3.3\sigma/S$. The LOD of a PDA sensor was estimated to be 10 ppm, which is sufficient to detect the dissolved ammonia in a liquid environment. Concerning the pH response of the PDA sensor, the ammonia solution pH in the range of 5–200 ppm concentration was investigated using a digital pH meter (Lab855 SI Analytics, Xylem). The pH of the employed solution varies from ~ 8.8 (5 ppm ammonia solution) to ~ 10.0 (200 ppm ammonia solution) as demonstrated in Figure S4. The sensor exhibits a color change under base solution testing, while no color response was observed for acid solution (Figure S5).

From the observation of the naked eye, the color of PDA vesicles gradually changed from blue to red as the ammonia concentration increased. The blue color indicates a controlled PDA sensor, dark violet indicates an ammonia concentration of

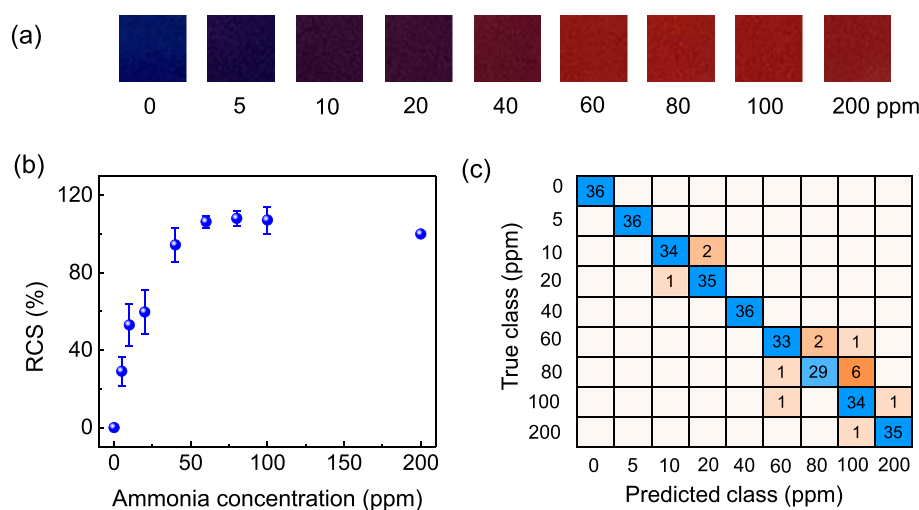


Figure 6. Digital CR of PDA sensors when exposed to different ammonia concentrations using (a) images captured by iPhone SE and their corresponding (b) red chromatic response and (c) SVM confusion matrix.

5–20 ppm, light violet color for 40–60 ppm ammonia, and red color for ammonia concentrations higher than 60 ppm (Figure 5a). The quantitative color change of the PDA sensors in the presence of ammonia was investigated by digital colorimetric analysis using RGB values from the scanner images, which are expressed in terms of an RCS, $RCS = [(r_{\text{sample}} - r_0)/(r_{\text{max}} - r_0)] \times 100$. The red chromaticity (r) was obtained by $r = R/(R + G + B)$, where R, G, and B are the intensities of three primary color components: red, green, and blue. In this experiment, the red chromaticity of PDA in the blue phase (r_0) and the PDA sample of interest (r_{sample}) are achieved as the PDA sample before and after incubating in the presence of interested ammonia concentration. r_{max} is the red-phase PDA after PDA exposure to 200 ppm ammonia concentration for 2 h. The RCS value exhibited an exponential increase with ammonia concentration as shown in Figure 5b. However, the concentration-dependent color change was less distinguishable at high ammonia levels. Therefore, a significant variance of CR values for each ammonia concentration may affect the accuracy of the simply predictive model. To address such an issue, machine learning for colorimetric analysis is proposed.

Here, an SVM and principal component analysis (PCA) were used as the machine learning classifier for training and assessing the performance of colorimetric detection. Four extracted features, including the mean value of red, green, and blue intensities and the RCS value of sample spot images, were used as the input parameters for machine learning classifiers. To investigate the color uniformity within the border of the detection zone, 12 selected areas for each image were used to test the performance of the machine learning model. Each ammonia concentration is tested 3 times, and three sets of PDA sensors were used to ensure the reliability of the data collection. The 108 samples of each ammonia concentration are randomly split into two groups with a ratio of 3:1 (81 training samples and 27 testing samples). PCA was used to extract the features of the data set before classifying the cluster by an SVM. The PCA score plot of the first two PCs of the PDA sensor to different ammonia concentrations is shown in Figure 5c. The first two PCs represented 99.11 and 0.74% of the variation, respectively. The PCA score plot generated using these two PCs accounted for 99.85% of variance explained in the measurements and showed an apparent data clustering. As

indicated in the result, we can discriminate between the similar color change of ammonia detection in the range of 5–200 ppm, except for the testing condition of 40 and 60 ppm.

To classify the ammonia concentration using the colorimetric image of the PDA sensor, the SVM with a Gaussian kernel function was utilized. Following the feature extraction by the PCA process, the multiclass SVM classifier extended from a binary class SVM classifier through the one-to-one approach is used to classify a group of nine ammonia concentrations. The performance of the SVM classifier was evaluated in terms of the confusion matrix, which represented the correlation between the actual (true) and predicted ammonia concentrations. The SVM shows excellent performance on the classification of ammonia concentration with 100% accuracy. As can be seen in Figure 5d, the misclassified pattern was not observed. We also investigated the effect of scanner sensors and their optics' effect on colorimetric analysis, including Epson V370 and Epson V600 photo scanners. As shown in Figure S6, slight differences in color intensity and red chromatic response were observed. However, by using eight features extracted from RGB intensity and RCS values of both scanner models, the SVM classifier showed an excellent accuracy of 100% for classifying the ammonia concentration. These results indicate that our PDA-based colorimetric sensor with a machine learning classifier can be a perfect tool for identifying ammonia levels in the range of 5–200 ppm.

In practical applications, immediate on-site detection of ammonia concentration using mobile colorimetric sensors is important. Hence, we applied our sensor and classifier model to the images captured by a smartphone. Figure 6a shows the colorimetric images acquired by the PDA sensor in the presence of ammonia with the concentration ranging from 5 to 200 ppm. A blue to dark purple and red transition was observed as the ammonia concentration increased. The red chromatic responses can identify the low content of ammonia in water below 60 ppm (Figure 6b). However, some errors might occur for ammonia concentrations between 10 and 20 ppm and for concentrations higher than 60 ppm. Therefore, to enhance the detectability, four extracted features of 144 samples (12 selected areas \times 3 testing times \times 4 sensor sets) of each ammonia concentration are randomly split into two groups at a ratio of 3:1 (108 training samples and 36 testing

samples). The PCA score plot generated using two PCs accounted for 98.47% of variance, as shown in Figure S7. A large distribution of images was observed for each class of ammonia concentration owing to the poor uniformity of RGB intensities of the test samples captured by the smartphone. In addition, the overlapping area was observed for the ammonia concentration between 10 and 20 ppm and for concentrations higher than 40 ppm. However, the SVM with a Gaussian kernel and the feature extraction process by PCA performed well in determining the nine classes of ammonia concentration with 95.1% accuracy. The confusion matrix showed 5.6 and 2.8% missed classification for 10 and 20 ppm (Figure 6c), respectively. The most missed prediction was found for 80 ppm ammonia with an actual positive rate of 80.6% due to colorimetric intensity from its nearest classes. The results demonstrate the potential of the PDA sensors and machine learning model to obtain a high accuracy of dissolved ammonia concentration. However, the classification accuracy rate strongly depends on image source quality, such as the file format, camera sensor, and optics. Further studies will improve the machine learning classifier by taking the images using different camera sensors and under various illumination conditions. The image processing algorithms can also detect signal noising or select features before transfer to the classifier. Moreover, the training data sets can be transferred to a smartphone app for on-site and real-time monitoring of dissolved ammonia in a water environment.

4. CONCLUSIONS

Here, colorimetric dissolved ammonia sensors were developed using a green chemical synthesized PDA vesicle. It was found that the morphology and the light absorption properties of PDA vesicles were changed once exposed to ammonia. Also, the CR of the PDA sensor increased when the ammonia concentration increased, showing a detection limit of 10 ppm and a response time of 20 min. In addition, the PDA sensor exhibited high stability at room temperature. Furthermore, we proposed the machine learning model that can automatically classify the ammonia concentration using the images captured by a scanner and a smartphone. By using the SVM classifier, a high dissolved ammonia concentration was possible, demonstrating that the proposed platform can be potentially utilized as a portable intelligent system with high accuracy, timely on-site detection, and real-time ammonia monitoring.

■ ASSOCIATED CONTENT

SI Supporting Information

The Supporting Information is available free of charge at <https://pubs.acs.org/doi/10.1021/acsomega.2c01419>.

FTIR spectra of the PDA sensor before and after exposure to 100 ppm ammonia; optical absorption spectra of the PDA sensor in the presence of different stimuli solutions and under various environmental temperature; pH values of ammonia concentration for testing solutions and sensing response to different pH buffers of PDA sensors; digital CR of the PDA sensor in the presence of different ammonia concentration captured images by two scanners; and score plot of nine concentrations of ammonia using colorimetric PDA images captured by a smartphone (PDF)

■ AUTHOR INFORMATION

Corresponding Author

Rawat Jaisutti – Department of Physics, Faculty of Science and Technology and Research Unit in Innovative Sensors and Nanoelectronic Devices, Thammasat University, Pathumthani 12121, Thailand; orcid.org/0000-0003-0461-9233; Email: jrawat@tu.ac.th

Authors

Papaorn Siribunbandal – Department of Physics, Faculty of Science and Technology and Research Unit in Innovative Sensors and Nanoelectronic Devices, Thammasat University, Pathumthani 12121, Thailand

Yong-Hoon Kim – School of Advanced Materials Science and Engineering, Sungkyunkwan University, Suwon 16419, Korea

Tanakorn Osothachan – Department of Physics, Faculty of Science, Mahidol University, Bangkok 10400, Thailand

Zhigang Zhu – School of Health Science and Engineering, University of Shanghai for Science and Technology, Shanghai 200093, China

Complete contact information is available at:

<https://pubs.acs.org/10.1021/acsomega.2c01419>

Notes

The authors declare no competing financial interest.

■ ACKNOWLEDGMENTS

The authors gratefully acknowledge the financial support provided by the Faculty of Science and Technology, Thammasat University, contact no SciGR 17/2565. R.J. thank Thammasat University for supporting Research Unit in Innovative Sensors and Nanoelectronic Devices. We are thankful to the Scientific Equipment Center and Department of Materials Science at the Faculty of Science, Kasetsart University, for using their equipment.

■ REFERENCES

- (1) U.S. Environmental Protection Agency. *Aquatic Life Ambient Water Quality Criteria for Ammonia-Freshwater 2013*, <https://www.epa.gov/sites/default/files/2015-08/documents/aquatic-life-ambient-water-quality-criteria-for-ammonia-freshwater-2013.pdf> (accessed Aug 01, 2013).
- (2) Löscher, C. R.; Kock, A.; Könneke, M.; LaRoche, J.; Bange, H. W.; Schmitz, R. A. Production of Oceanic Nitrous Oxide by Ammonia-Oxidizing Archaea. *Biogeosciences* **2012**, *9*, 2419–2429.
- (3) Fan, Y. Z.; Dong, J. X.; Zhang, Y.; Li, N.; Liu, S. G.; Geng, S.; Ling, Y.; Luo, H. Q.; Li, N. B. A Smartphone-Coalesced Nanoprobe for High Selective Ammonia Sensing Based on the pH-Responsive Biomass Carbon Nanodots and Headspace Single Drop Microextraction. *Spectrochim. Acta Mol. Biomol. Spectrosc.* **2019**, *219*, 382–390.
- (4) Environmental Protection Agency. *Final Aquatic Life Ambient Water Quality Criteria For Ammonia-Freshwater 2013*, <https://www.govinfo.gov/content/pkg/FR-2013-08-22/pdf/2013-20307.pdf> (accessed Aug 01, 2013).
- (5) Zhou, L.; Boyd, C. E. Comparison of Nessler, Phenate, Salicylate and Ion Selective Electrode Procedures for Determination of Total Ammonia Nitrogen in Aquaculture. *Aquac* **2016**, *450*, 187–193.
- (6) LeDuy, A.; Samson, R. Testing of An Ammonia Ion Selective Electrode for Ammonia Nitrogen Measurement in the Methanogenic Sludge. *Biotechnol. Lett.* **1982**, *4*, 303–306.
- (7) Ling, T. L.; Ahmad, M.; Heng, L. Y. An Amperometric Biosensor Based on Alanine Dehydrogenase for the Determination of Low Level of Ammonium Ion in Water. *J. Sens.* **2011**, *2011*, 980709.

- (8) Werkmeister, F. X.; Koide, T.; Nickel, B. A. Ammonia Sensing for Enzymatic Urea Detection using Organic Field Effect Transistors and a Semipermeable Membrane. *J. Mater. Chem. B* **2016**, *4*, 162–168.
- (9) Strobl, M.; Walcher, A.; Mayr, T.; Klimant, I.; Borisov, S. M. Trace Ammonia Sensors Based on Fluorescent Near-Infrared-Emitting aza-BODIPY Dyes. *Anal. Chem.* **2017**, *89*, 2859–2865.
- (10) Dong, J. X.; Gao, Z. F.; Zhang, Y.; Li, B. L.; Li, N. B.; Luo, H. Q. A Selective and Sensitive Optical Sensor for Dissolved Ammonia Detection via Agglomeration of Fluorescent Ag Nanoclusters and Temperature Gradient Headspace Single Drop Microextraction. *Biosens. Bioelectron.* **2017**, *91*, 155–161.
- (11) Cho, Y. B.; Jeong, S. H.; Chun, H.; Kim, Y. S. Selective Colorimetric Detection of Dissolved Ammonia in Water via Modified Berthelot's Reaction on Porous Paper. *Sens. Actuators, B* **2018**, *256*, 167–175.
- (12) Jayawardane, B. M.; McKelvie, I. D.; Kolev, S. D. Development of a Gas-Diffusion Microfluidic Paper-Based Analytical Device (μ PAD) for the Determination of Ammonia in Wastewater Samples. *Anal. Chem.* **2015**, *87*, 4621–4626.
- (13) Nichols, M. L.; Willits, C. O. Reactions of Nessler's Solution. *J. Am. Chem. Soc.* **1934**, *56*, 769–774.
- (14) Patton, C. J.; Crouch, S. R. Spectrophotometric and Kinetics Investigation of the Berthelot Reaction for the Determination of Ammonia. *Anal. Chem.* **1977**, *49*, 464–469.
- (15) Nguyen, T.-H.; Mugheri, L.; Rivron, C.; Tran-Thi, T.-H. Innovative Colorimetric Sensors for the Selective Detection of Monochloramine in Air and in Water. *Sens. Actuators, B* **2015**, *208*, 622–627.
- (16) Searle, P. L. The Berthelot or Indophenol Reaction and Its Use in the Analytical Chemistry of Nitrogen. A review. *Analyst* **1984**, *109*, 549–568.
- (17) Ngo, T. T.; Phan, A. P. H.; Yam, C. F.; Lenhoff, H. M. Interference in Determination of Ammonia with the Hypochlorite-Alkaline Phenol Method of Berthelot. *Anal. Chem.* **1982**, *54*, 46–49.
- (18) Dolai, S.; Bhunia, S. K.; Beglaryan, S. S.; Kolusheva, S.; Zeiri, L.; Jelinek, R. Colorimetric Polydiacetylene–Aerogel Detector for Volatile Organic Compounds (VOCs). *ACS Appl. Mater. Interfaces* **2017**, *9*, 2891–2898.
- (19) Phonchai, N.; Khanantong, C.; Kielar, F.; Traiphon, R.; Traiphon, N. Low-Temperature Reversible Thermochromic Polydiacetylene/Zinc(II)/Zinc Oxide Nanocomposites for Colorimetric Sensing. *ACS Appl. Nano Mater.* **2019**, *2*, 4489–4498.
- (20) Jannah, F.; Kim, J.-M. pH-Sensitive Colorimetric Polydiacetylene Vesicles for Urease Sensing. *Dyes Pigm.* **2019**, *169*, 15–21.
- (21) Weston, M.; Kuchel, R. P.; Ciftci, M.; Boyer, C.; Chandrawati, R. A Polydiacetylene-based Colorimetric Sensor as An Active Use-by Date Indicator for Milk. *J. Colloid Interface Sci.* **2020**, *572*, 31–38.
- (22) Yapor, J. P.; Alharby, A.; Gentry-Weeks, C.; Reynolds, M. M.; Alam, A. K. M. M.; Li, Y. V. Polydiacetylene Nanofiber Composites as a Colorimetric Sensor Responding To *Escherichia Coli* and pH. *ACS Omega* **2017**, *2*, 7334–7342.
- (23) Weston, M.; Ciftci, M.; Kuchel, R. P.; Boyer, C.; Chandrawati, R. Polydiacetylene for the Detection of α -Hemolysin in Milk toward the Diagnosis of Bovine Mastitis. *ACS Appl. Polym. Mater.* **2020**, *2*, 5238–5248.
- (24) Khanantong, C.; Charoenthai, N.; Phuangkaew, T.; Kielar, F.; Traiphon, N.; Traiphon, R. Phase Transition, Structure and Color-Transition Behaviors of Monocarboxylic Diacetylene and Polydiacetylene Assemblies: The Opposite Effects of Alkyl Chain Length. *Colloids Surf. A Physicochem. Eng. Asp.* **2018**, *553*, 337–348.
- (25) Nguyen, L. H.; Naficy, S.; McConchie, R.; Dehghani, F.; Chandrawati, R. Polydiacetylene-based Sensors to Detect Food Spoilage at Low Temperatures. *J. Mater. Chem. C* **2019**, *7*, 1919–1926.
- (26) Park, J. H.; Choi, H.; Cui, C.; Ahn, D. J. Capillary-Driven Sensor Fabrication of Polydiacetylene-on-Silica Plate in 30 Seconds: Facile Utilization of π -Monomers with C18- to C25-Long Alkyl Chain. *ACS Omega* **2017**, *2*, 7444–7450.
- (27) Park, S.; Lee, G. S.; Cui, C.; Ahn, D. J. Simple Detection of Food Spoilage using Polydiacetylene/Poly(vinyl alcohol) Hybrid Films. *Macromol. Res.* **2016**, *24*, 380–384.
- (28) Park, D.-H.; Heo, J.-M.; Jeong, W.; Yoo, Y. H.; Park, B. J.; Kim, J.-M. Smartphone-Based VOC Sensor Using Colorimetric Polydiacetylenes. *ACS Appl. Mater. Interfaces* **2018**, *10*, 5014–5021.
- (29) Li, Q.; Ren, S.; Peng, Y.; Lv, Y.; Wang, W.; Wang, Z.; Gao, Z. A Colorimetric Strip for Rapid Detection and Real-Time Monitoring of Histamine in Fish Based on Self-Assembled Polydiacetylene Vesicles. *Anal. Chem.* **2020**, *92*, 1611–1617.
- (30) Akkaynak, D.; Treibitz, T.; Xiao, B.; Gürkan, U. A.; Allen, J. J.; Demirci, U.; Hanlon, R. T. Use of Commercial Off-the-Shelf Digital Cameras for Scientific Data Acquisition and Scene-Specific Color Calibration. *J. Opt. Soc. Am. A* **2014**, *31*, 312–321.
- (31) Mutlu, A. Y.; Kılıç, V.; Özdemir, G. K.; Bayram, A.; Horzum, N.; Solmaz, M. E. Smartphone-based Colorimetric Detection via Machine Learning. *Analyst* **2017**, *142*, 2434–2441.
- (32) Mercan, Ö. B.; Kılıç, V.; Şen, M. Machine Learning-based Colorimetric Determination of Glucose in Artificial Saliva with Different Reagents using a Smartphone Coupled μ PAD. *Sens. Actuators, B* **2021**, *329*, 129037.
- (33) Solmaz, M. E.; Mutlu, A. Y.; Alankus, G.; Kılıç, V.; Bayram, A.; Horzum, N. Quantifying Colorimetric Tests using a Smartphone App based on Machine Learning Classifiers. *Sens. Actuators, B* **2018**, *255*, 1967–1973.
- (34) Sajed, S.; Kolahdouz, M.; Sadeghi, M. A.; Razavi, S. F. High-Performance Estimation of Lead Ion Concentration Using Smartphone-Based Colorimetric Analysis and a Machine Learning Approach. *ACS Omega* **2020**, *5*, 27675–27684.
- (35) Luka, G. S.; Nowak, E.; Kawchuk, J.; Hoorfar, M.; Najjaran, H. Portable Device for the Detection of Colorimetric Assays. *R. Soc. Open Sci.* **2017**, *4*, 171025.
- (36) Helfer, G. A.; Barbosa, J. L. V.; Alves, D.; da Costa, A. B.; Beko, M.; Leithardt, V. R. Q. Multispectral Cameras and Machine Learning Integrated into Portable Devices as Clay Prediction Technology. *J. Sens. Actuator Netw.* **2021**, *10*, 40.
- (37) Cho, E.; Kim, H.; Choi, Y.; Paik, S. R.; Jung, S. Polydiacetylenyl β -Cyclodextrin based Smart Vesicles for Colorimetric Assay of Arginine and Lysine. *Sci. Rep.* **2016**, *6*, 31115.
- (38) Valdez, M.; Gupta, S. K.; Lozano, K.; Mao, Y. ForceSpun Polydiacetylene Nanofibers as Colorimetric Sensor for Food Spoilage Detection. *Sens. Actuators, B* **2019**, *297*, 126734.
- (39) Kim, J.-M.; Lee, J.-S.; Choi, H.; Sohn, D.; Ahn, D. J. Rational Design and in-Situ FTIR Analyses of Colorimetrically Reversible Polydiacetylene Supramolecules. *Macromolecules* **2005**, *38*, 9366–9376.
- (40) Zhang, Z.; Wei, T.; Chen, Y.; Chen, T.; Chi, B.; Wang, F.; Chen, X. A Polydiacetylenes-based Colorimetric and Fluorescent Probe for L-Arginine and L-Lysine and Its Application for Logic Gate. *Sens. Actuators, B* **2018**, *255*, 2211–2217.